Journal of Pharmacokinetics and Pharmacodynamics, Vol. 33, No. 2, April 2006 (© 2006)
DOI: 10.1007/s10928-006-9007-3

Pharmacodynamic Models for Agents that Alter Production of Natural Cells with Various Distributions of Lifespans[1]

Wojciech Krzyzanski,[2,3] Sukyung Woo,[2] William J Jusko[2]

Received March 17, 2005—Final January 20, 2006—Published Online March 25, 2006

Indirect pharmacodynamic response (IDR) models were developed for agents which alter the generation of cell populations with arbitrary lifespan distributions. These models extend lifespan based IDR models introduced previously [J. Pharmacokinet. Biopharm. 27: 467, 1999] for cell populations with the same lifespan ("delta" distribution). Considered are cell populations exhibiting time-invariant lifespan distributions described by the probability density function $\ell(\tau)$. It is assumed that cell response (R) is produced at a zero-order rate ($k_{in}(t)$) and is eliminated from the population when the cell lifespan expires. The cell loss rate is calculated as $k_{in} * \ell(t)$, where '$*$' denotes the convolution operator. Therapeutic agents can stimulate or inhibit production rates according to the Hill function: $1 \pm H(C(t))$ where $H(C(t))$ contains the capacity (S_{max}) and potency (SC_{50}) parameters and $C(t)$ is a pharmacokinetic function. The production rate is $k_{in}(t) = k_{in} \cdot [1 \pm H(C(t))]$. The operational model is $dR/dt = k_{in}(t) - k_{in} * \ell(t)$ with the baseline condition $R_0 = k_{in} \cdot T_R$, where T_R is the mean lifespan. Single populations as well as populations with precursors were examined by simulation to establish the role of lifespan distribution parameters (mean and standard deviation) in controlling the response vs. time profile. Estimability of parameters was assessed. Numerical techniques of solving differential equations with the convolution integral were proposed. In addition, the models were applied to literature data to describe the stimulatory effects of single doses of recombinant human erythropoietin on reticulocytes in blood. The estimates of S_{max} and SC_{50} for these agents were obtained along with means and standard deviations for reticulocyte lifespan distributions. The proposed models can be used to analyze the pharmacodynamics of agents which alter natural cell production yielding parameters describing their efficacy and potency as well as means and standard deviations for cell lifespan distributions.

KEY WORDS: indirect response models; pharmacodynamics; cell lifespans; convolution; erythropoietin.

[1] This work was supported in part by Grant No. GM 57980 from the National Institute of General Medical Sciences, National Institutes of Health.
[2] Department of Pharmaceutical Sciences, University at Buffalo, State University of New York, Buffalo, New York 14260, USA
[3] To whom correspondence should be addressed. Telephone:+1-716-645-2842 ext. 257; fax: +1-716-645-3693; e-mail: wk@buffalo.edu

INTRODUCTION

Cell populations of pharmacological interest are those affected by drugs with therapeutic or toxic effects. Hematopoietic cells, neoplastic cells, parasites and bacteria are examples. Mathematical models that describe population size as a function of time after exposure to a therapeutic agent become increasingly important in rational design of various treatments against cancer, bacterial infection and many others. Turnover models combine the physiology of treated organisms with the pharmacology of the administered drugs. The most common technique employs compartmental models where various pools represent different cell populations and cells are transferred between compartments at first-order rates (1,2). Recognition of cell aging or maturation led to development of cell kinetic models where primary entities were distributions of age (3,4). First-order cell loss was a key process in both of these approaches. Models of cell turnover incorporating senescence as a mechanism of cell removal have been developed (5–7). Only the simplest point cell lifespan distributions with a single parameter (the mean cell lifespan) were considered. The continuous distribution of cell lifespans has been utilized in analysis of tracer cell kinetic data (8,9). It was assumed that tracer radioactivity represented the probability that a certain number of cells would survive up to a given age that could be calculated from the cumulative lifespan distribution (10–12). Nonparametric methods of determination of the mean lifespan and standard deviation from cell survival data have been developed for RBC (13) and platelets (14). Various parametric models for lifespan distribution of RBC and platelets have been proposed (10,15,16). Such models have been combined with PD models where the primary response consisted of cell count (1). In the absence of cell survival data the lifespan distribution parameters have been estimated from cell count data along with other PD parameters (17). We apply this methodology in the following report.

The purpose of this paper is to apply the PD modeling approaches introduced previously (1,17) and extend the formalism we introduced for single lifespan cell populations to more realistic cell lifespans distributions (6). We investigate the role of continuously distributed lifespan in characterization of cell kinetics for hematopoietic populations stimulated by growth factors. An indirect mechanism of drug action is assumed with two parameters describing drug efficacy ($S_{\max}$) and potency (SC_{50}) (18). We also study the feasibility of estimating lifespan distribution parameters (mean and standard deviation) for commonly accepted probability density functions for hematopoietic cell populations (10,15,16). The limitations of available software for pharmacokinetic and pharmacodynamic (PK/PD) data analysis regarding incorporation of the convolution integral

into a model described by differential equations prompted us to develop numerical techniques that can solve the model equations using existing commercially available software. We have not tested applicability of previously introduced programs created for pharmacokinetic models with the convolution operator (19). Our model was evaluated by analysis of stimulatory effect of recombinant human erythropoietin (rHuEPO) using literature data (20).

THEORETICAL

A fundamental assumption is that every cell in the population is assigned a unique lifespan. If the age of a cell reaches its lifespan, then the cell has to leave the population. The most natural example is cell senescence, where the cell death determines its lifespan as the duration of the aging process. However, other mechanisms of cell loss can be interpreted as expiration of the lifespan. If cell loss is lifespan based, then cells of the same age will leave the population at the same time. In the most simplistic case, all cells have the same lifespan (i.e., point distribution). A more realistic assumption would be that the lifespan is continuously distributed and characterized by a probability density function (p.d.f.) $\ell(\tau)$ where the probability of finding a cell in the population with the lifespan smaller than t can be calculated as:

$$P(\tau \leq t) = \int_0^t \ell(\tau) d\tau \tag{1}$$

This assumption makes the lifespan a random variable defined for a given cell population. The mean lifespan (T) and standard deviation (SD) for its distribution are (16)

$$T = \int_0^\infty \tau \ell(\tau) d\tau \quad \text{and} \quad SD = \left(\int_0^\infty (\tau - T)^2 \ell(\tau) d\tau \right)^{1/2} \tag{2}$$

Our next assumption is that the lifespan distribution is time independent. Although realistically one should consider changes in lifespan distribution due to external factors (disease, toxicity, drug therapy, etc.), analysis of such circumstances will require much more complex formalism falling out of the present scope. This assumption is based on the stationarity principle applied to lifespan distribution parameters considered as pharmacodynamic parameters. However, one must be aware of potential

bias introduced to estimates of such parameters should this principle be violated.

The cell turnover in the population is determined by two processes: production and loss (see Fig. 1). If the production rate $k_{\text{in}}(t)$ and loss rate $k_{\text{out}}(t)$ are functions of time, then the change in the cell number N is determined by the following equation:

$$\frac{dN}{dt} = k_{\text{in}}(t) - k_{\text{out}}(t) \tag{3}$$

The assumption that each cell exits the population when its lifespan expires allows one to determine k_{out}(t) if the lifespan distribution is known (see Appendix A):

$$k_{\text{out}}(t) = \int_0^\infty k_{\text{in}}(t-\tau)\ell(\tau)d\tau \tag{4}$$

Since for negative lifespans the p.d.f. $\ell(\tau) = 0$, the integral in Eq. (4) can be written as the convolution of $k_{\text{in}} * \ell(t)$ and Eq. (3) can be simplified

$$\frac{dN}{dt} = k_{\text{in}}(t) - k_{\text{in}} * \ell(t) \tag{5}$$

Note that for the delta distribution of the lifespan $\ell(\tau) = \delta(\tau - T)$, the convolution in Eq. (5) creates a delay in time

$$k_{\text{in}} * \ell(t) = k_{\text{in}}(t - T) \tag{6}$$

and Eq. (5) reduces to the single lifespan model introduced previously (6). For most model applications it will be assumed that prior to any perturbation of the cell population (e.g., by drug treatment), the system will remain in steady-state with a constant rate of cell production $k_{\text{in}}(t) \equiv k_{\text{in0}}$ for $t < 0$. Then, one can determine the baseline number of cells N_0 (see Appendix B)

$$N_0 = k_{\text{in0}} \cdot T \tag{7}$$

If the production rate is stimulated or inhibited by a drug, then for $t \geq 0$

$$k_{\text{in}}(t) = k_{\text{in0}} \cdot \left(1 \pm \frac{E_{\max} \cdot C(t)}{EC_{50} + C(t)}\right) \tag{8}$$

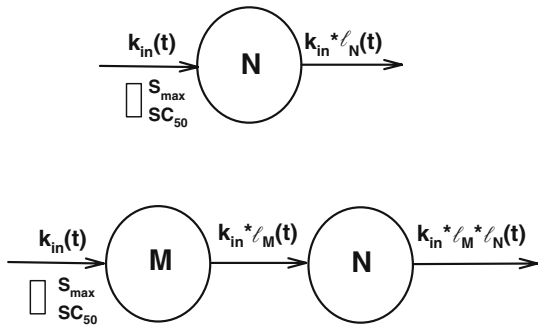

Fig. 1. Schematic diagrams representing the basic LIDR model (upper) and basic LIDR model with a precursor pool (lower). The cells are produced at a constant rate k_{in0}. A drug stimulates the production rate via the Hill function (open box) characterized by the parameters S_{max} and SC_{50}. The product k_{in0} and the Hill function is represented by the time dependent function $k_{in}(t)$. The cells exit the population after their lifespan expires. The cell loss rate is determined by the convolution of $k_{in}(t)$ with the p.d.f. for the lifespan distribution $\ell_N(t)$. For the precursor model, the input rate to the central pool N is the output rate from the precursor pool $k_{in} * \ell_M(t)$. The elimination rate from the central pool is determined by the convolution of $k_{in} * \ell_M(t)$ with $\ell_N(t)$.

where '+' is for stimulation and '−' for inhibition. Here $C(t)$ denotes the drug concentration at the site of action, E_{max} is the maximum effect and EC_{50} stands for drug concentration eliciting 50% of maximum effect (18). Eq. (8) is valid for negative times if $C(t) = 0$, for $t < 0$. Eq. (5) with $k_{in}(t)$ described by Eq. (8) constitutes the basic lifespan based indirect response model (LIDR).

If there is a precursor pool for the cell population (M), then Eq. (5) would apply to describe the number of cells

$$\frac{dM}{dt} = k_{in}(t) - k_{in} * \ell_M(t) \tag{9}$$

Here $k_{in}(t)$ denotes the precursor cell production rate and $\ell_M(\tau)$ is the p.d.f. for precursor cell lifespan distribution. If each cell that exits the precursor enters the successor pool, then loss rate for cells M coincides with the production rate for cells N. Consequently,

$$\frac{dN}{dt} = k_{in} * \ell_M(t) - k_{in} * \ell_M * \ell_N(t) \tag{10}$$

$\ell_N(\tau)$ is the p.d.f. for the lifespan distribution for cells in the central pool. The baseline conditions for the precursor (M_0) and central pools (N_0) become:

$$M_0 = k_{in0} \cdot T_M \quad \text{and} \quad N_0 = k_{in0} \cdot T_N \tag{11}$$

where T_M and T_N denote the means of lifespan distributions for M and N. Eq. (11) can be derived similarly to Eq. (7). If a drug inhibits or stimulates the production of the precursor cells, then Eq. (8) should be used in the convolution terms in Eq. (9) and (10).

METHODS

Calculation of the Convolution Operator for Various Lifespan Distributions

The proposed models contain the convolution operator that is not implemented into standard PK/PD software packages. Our approach was to develop a technique that allows one to calculate the convolution of arbitrary functions using ordinary differential equations which are available in PK/PD software. If the p.d.f. for the lifespan distribution $\ell(\tau)$ is a specific function (e.g., poly-exponential, polynomial, or gamma), then the convolution with $k_{\text{in}}(t)$ can be exactly calculated. For arbitrary p.d.f. (e.g., lognormal) we provide an approximation. Below we present the equations allowing one to calculate the convolution integrals for lifespan distribution described by the gamma function (15, 16) and Dornhorst function (10). We also demonstrate how to calculate the convolution integral for an arbitrary p.d.f. using the frequency histogram as an approximation.

Let $\ell_n(\tau)$ denote the gamma distribution

$$\ell_n(\tau) = \frac{1}{\tau_0}\frac{(\tau/\tau_0)^{n-1}}{(n-1)!}e^{-(\tau/\tau_0)} \tag{12}$$

Eq. (12) has been introduced to describe the platelet lifespan distribution in the multiple-hit model (15, 16). The basic mechanism for platelet removal from the circulation is random collisions (hits) with walls of blood vessels or other circulating cells. The parameter τ_0 denotes the mean time between hits and n is the number of hits. The convolution can be calculated as

$$k_{\text{in}} * \ell_n(t) = X_n \tag{13}$$

where the dummy variables X_i $(i = 1, \ldots, n)$ satisfy the following ordinary differential equations:

$$\frac{dX_1}{dt} = \frac{1}{\tau_0}k_{\text{in}}(t) - \frac{1}{\tau_0}X_1, \quad X_1(0) = k_{\text{in}0} \tag{14}$$

and for $i = 2, \ldots, n$

$$\frac{dX_i}{dt} = \frac{1}{\tau_0}X_{i-1} - \frac{1}{\tau_0}X_i, \quad X_i(0) = k_{\text{in}0} \tag{15}$$

The case $n = 1$, reduces $\ell_n(\tau)$ to the mono-exponential p.d.f. that describes distribution of cell lifespans for a population exposed to a random destruction. For derivations see Appendix C.

The Dornhorst model of RBC survival assumes that erythrocytes are randomly removed from the circulation up to time T_R (their common lifespan) when they die due to senescence (10). Then the distribution function Eq. (1) becomes

$$P(\tau \leq t) = \theta(T_R - t)e^{-\lambda t} \tag{16}$$

where λ denotes the random killing rate constant and $\theta(t)$ is the Heaviside step function $\theta(t) = 1$, if $t \geq 0$, and $\theta(t) = 0$ otherwise. Consequently, the p.d.f. for the Dornhorst RBC lifespan distribution is

$$\ell_D(\tau) = \delta(T_R - \tau)e^{-\lambda T_R} + \lambda\theta(T_R - \tau)e^{-\lambda t} \tag{17}$$

The convolution can be calculated as follows

$$k_{\text{in}} * \ell_D(t) = k_{\text{in}}(t - T_R)e^{-\lambda T_R} + \lambda X(t) \tag{18}$$

where the dummy variable X satisfies the following differential equation

$$\frac{dX}{dt} = k_{\text{in}}(t) - k_{\text{in}}(t - T_R)e^{-\lambda T_R} - \lambda X, \quad X(0) = \frac{k_{\text{in}0}}{\lambda}\left(1 - e^{-\lambda T_R}\right) \tag{19}$$

For derivations see Appendix C. In the case of the model with the precursor pool one needs to calculate the double convolution in Eq. (10). This can be reduced to calculation of single convolutions if $k_{\text{in}}(t)$ in the above equations is replaced by $k_{\text{in}} * \ell_M(t)$, since for $t < 0$ $k_{\text{in}} * \ell_M(t) \equiv k_{\text{in}0}$.

Below we present a way of calculation of the convolution integral Eq. (4) for any p.d.f. that is described by an explicit continuous function. Our approach is based on an approximation of the continuous p.d.f. with a histogram of known a priori number of bins (n). Then the convolution integral can be calculated for the histogram p.d.f. If n becomes sufficiently large and the bin width decreases with n, then the error for such an approximation becomes small. Let $\tau_1 = 0 < \tau_2 < \cdots < \tau_{n+1}$ denote the limits for the bins. If one chooses the same width $\Delta\tau$ for each bin, then $\tau_i = (i-1)\Delta\tau, i = 1, \ldots, n+1$. The height of the ith bar of the histogram can be calculated as

$$a_i = \frac{\alpha_i}{\alpha_1(\tau_2 - \tau_1) + \cdots + \alpha_n(\tau_{n+1} - \tau_n)} \quad \text{where } \alpha_i = \ell((\tau_{i+1} + \tau_i)/2), \quad i = 1, \ldots, n \tag{20}$$

Then the histogram can be defined as

$$\ell_{\text{hist}}(\tau) = \sum_{i=1}^{n} a_i \theta(\tau - \tau_i)\theta(\tau_{i+1} - \tau) \tag{21}$$

Fig. 2 shows the plots of $\ell(\tau)$ and $\ell_{\text{hist}}(\tau)$ that illustrate how the approximation Eq. (20) works. If we introduce dummy variables $X_0, X_1, \ldots, X_{n+1}$ that satisfy the following system of differential equations

$$\frac{dX_i}{dt} = k_{\text{in}}(t) - k_{\text{in}}(t - \tau_i), \quad X_i(0) = k_{\text{in}0}\tau_i, \qquad i = 1, \ldots, n+1 \tag{22}$$

then

$$k_{\text{in}} * \ell_{\text{hist}}(t) = \sum_{i=1}^{n} a_i (X_{i+1} - X_i) \tag{23}$$

The derivation of Eq. (23) is shown in Appendix C. The mean and SD for the lifespan distribution described by $\ell_{\text{hist}}(\tau)$ can be calculated as follows

$$\begin{aligned} T_{\text{hist}} &= \frac{1}{2}\sum_{i=1}^{n} a_i \left(\tau_{i+1}^2 - \tau_i^2\right) \quad \text{and} \\ SD_{\text{hist}}^2 &= \frac{1}{3}\sum_{i=1}^{n} a_i \left((\tau_{i+1} - T_{\text{hist}})^3 - (\tau_i - T_{\text{hist}})^3\right) \end{aligned} \tag{24}$$

Simulations

A series of simulations was performed to investigate the role of continuous lifespan distribution parameters (mean, SD) in control of the response curve. The kinetic function was monoexponential

$$C = \frac{\text{Dose}}{V} e^{-k_{el}t} \tag{25}$$

where $V = 1, k_{el} = 0.1$. Because of the simplicity of calculations of the convolution operator, the gamma distribution p.d.f. Eq. (12) was used for simulations. The mean time (T) and standard deviation (SD) for such distributions are (16)

$$T = n \cdot \tau_0 \quad \text{and} \quad SD = \sqrt{n} \cdot \tau_0 \tag{26}$$

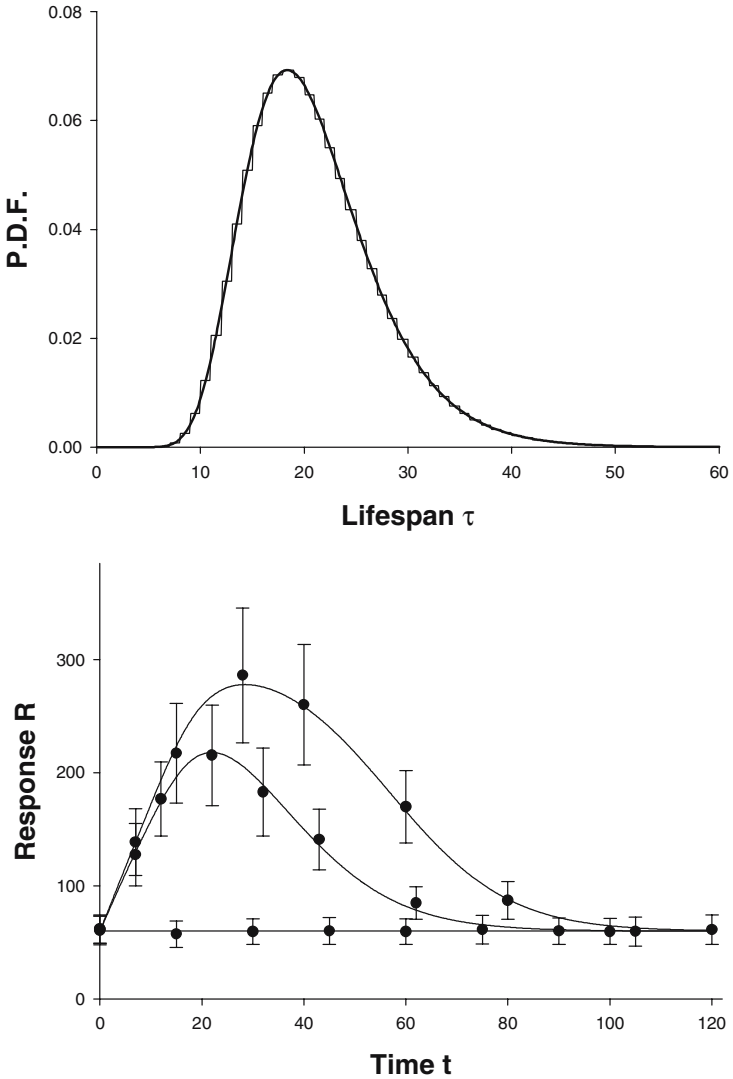

Fig. 2. Response vs. time profiles corresponding to the lognormal lifespan distribution. Upper panel: Plots of p.d.f. $\ell(\tau)$ (thick line) and $\ell_{\text{hist}}(\tau)$ (thin line) for lognormal lifespan distribution described by Eq. (31) and (21) with $m = 3, \sigma = 0.3, n = 60$, and $\Delta\tau = 1$. Lower panel: Response vs. time profiles for the basic LIDR model corresponding to the lifespan distribution described by $\ell_{\text{hist}}(\tau)$. The responses (lines) were generated for the PK function Eq. (25) at doses 100, 1000, and placebo. Remaining PK and PD parameters are listed in Table I. The symbols (•) indicate the mean values of the 100 individual erroneous response profiles with normally distributed noise generated according to the variance model Eq. (32). The bars denote the standard deviations.

The values for SD were selected such that for a given T, the parameter n in Eq. (26) became an integer.

The absolute cell number N in the central pool was scaled by the volume of the central pool V_c to obtain measurable responses

$$R = N/V_c \tag{27}$$

where $V_c = 1$. Then the differential equations for R in the basic model become

$$\frac{dR}{dt} = k_{\text{in}R} \cdot \left(1 + \frac{S_{\max} C(t)}{SC_{50} + C(t)}\right) - k_{\text{in}R} \cdot \left(1 + \frac{S_{\max} C}{SC_{50} + C}\right) * \ell_R(t) \tag{28}$$

and for the model with the precursor

$$\frac{dR}{dt} = k_{\text{in}R} \cdot \left(1 + \frac{S_{\max} C}{SC_{50} + C}\right) * \ell_P(t) - k_{inR} \cdot \left(1 + \frac{S_{\max} C}{SC_{50} + C}\right) * \ell_P * \ell_R(t) \tag{29}$$

where according to Eq. (7)

$$k_{\text{in}R} = R_0/T_R \tag{30}$$

The R_0 denotes the baseline value for R and was assumed $= 60$ throughout simulations. The T_R was the mean cell lifespan for the central pool. There was no need to solve a differential equation for M, since the M variable is not present in Eq. (29). The convolution operators were calculated according to Eqs. (13)–(15). The simulations were performed by ADAPT II (21).

Estimability of PD Parameters in the Basic LIDR Model

To verify if the PD parameters can be identified for a data set that consists of responses described by the basic LIDR model, an analysis of computer generated data was performed. Eq. (25) was used to simulate the PK function that was a driving force for the response R calculated at selected time points according to Eq. (28) with $S_{\max} = 4$ and $SC_{50} = 10$ and the baseline $R_0 = 60$. The lognormal distribution of cell lifespans were assumed (22)

$$\ell_{\log}(\tau) = \frac{1}{\sigma \tau \sqrt{2\pi}} e^{\frac{-(\ln \tau - m)^2}{2\sigma^2}} \tag{31}$$

with $m = 3$ and $\sigma = 0.3$. The convolution integral in Eq. (28) was calculated using approximation $\ell_{\text{hist}}(\tau)$ and Eqs. (22)–(23) where the number of bins $n = 60$ and $\Delta\tau = 1$. Both $\ell_{\log}(\tau)$ and $\ell_{\text{hist}}(\tau)$ are shown in Fig. 2. The responses were simulated at two dose levels of 100 and 1000 and placebo. There were 8 sampling times per dose selected to cover the entire response vs. time curve. Fig. 2 shows the response profiles. Residual variability normally distributed was introduced to generated responses according to the following variance model

$$Var(Y) = aY^b \tag{32}$$

where $a = 0.04$ and $b = 2$ and $Y = R$ was the predicted by the model response value. One hundred replicates of erroneous responses were simulated. Each replicate was fitted with the same model that has been used for generating the errorless responses and the PD parameters R_0, $S_{\max}$, SC_{50}, m, and σ were estimated. T_{mean}, SD, and $k_{\text{in}R}$ were secondary parameters. The maximum likelihood estimator was applied with the variance model Eq. (32) where a and b were fixed. The minimization procedure was considered successful if it converged and the estimated values were within (0.1 × (true value), 10 × (true value)) interval. No limits on parameters were imposed during estimation. Analysis was performed using ADAPT II (21). The mean prediction percent error (MPE) was used as a measure of bias (23)

$$\text{MPE} = \frac{\frac{1}{k}\sum_{j=1}^{k}(p_j - p)}{p}100 \tag{33}$$

where p_j is the estimated value of the parameter p for the jth data set and k denotes the number of successful minimizations. The root mean squared prediction percent error (RMSPE) was used as a measure of precision for parameter estimation (23).

$$\text{RMSPE} = \frac{\sqrt{\frac{1}{k}\sum_{j=1}^{k}(p_j - p)^2}}{p}100 \tag{34}$$

Stimulation of Reticulocyte Production by rHuEPO

The LIDR model with various lifespan distribution functions was applied to a previously analyzed data set (20) to examine the estimability of lifespan distribution parameters along with dynamic parameters of rHuEPO. Recombinant human erythropoietin mimics the endogenous hormone which is a major regulator of erythropoiesis. After binding to its

receptors expressed on early progenitor cells in the bone marrow, it stimulates their proliferation leading to increased reticulocyte numbers in the blood. The rHuEPO serum concentrations and reticulocyte counts were obtained at various times after subcutaneous administration of rHuEPO to healthy subjects (20). These data were also used to test a PK/PD model where fixed lifespans were assumed for precursor and central pools (6).

The PK data were described by the following equations as previously (6).

$$C_{\mathrm{EPO}}(t) = \begin{cases} C_0, & if\ \ t < 0 \\ C_0 + C_1\left(1 - e^{-k_1 t}\right), & if\ \ 0 \le t \le t_{\mathrm{lag}} \\ C_0 + C_1\left(e^{-k_1(t-t_{\mathrm{lag}})} - e^{-k_1 t}\right) + C_2\left(e^{-k_2(t-t_{\mathrm{lag}})} - e^{-k_2 t}\right), & if\ \ t > t_{\mathrm{lag}} \end{cases} \tag{35}$$

where t_{lag} denotes the time at which the zero-order absorption of rHuEPO ends and first-order absorption begins. The basic model with a precursor (Eq. 29) was used to describe the stimulatory effects of rHuEPO on reticulocytes. The progenitor cells in the bone marrow constituted the precursor (P) and the reticulocyte count expressed as the percent of RBC was the response (R). Since the simulations showed that the SD for the precursor cell lifespan distribution is poorly estimable, the delta distribution was applied for the precursor pool

$$\ell_P(\tau) = \delta(\tau - T_P) \tag{36}$$

where T_P denotes the precursor cell lifespan. Reticulocytes are considered a subpopulation of circulating erythrocytes; therefore the Dornhorst lifespan distribution (Eq. 20) was used for the reticulocyte lifespan distribution. Consequently, Eq. (29) became

$$\frac{dR}{dt} = k_{\mathrm{in}R} \cdot \left(1 + \frac{S_{\max} C_{\mathrm{del}}(t)}{SC_{50} + C_{\mathrm{del}}(t)}\right) - k_{\mathrm{in}R} \cdot \left(1 + \frac{S_{\max} C_{\mathrm{del}}}{SC_{50} + C_{\mathrm{del}}}\right) * \ell_R(t) \tag{37}$$

where

$$C_{\mathrm{del}}(t) = C_{\mathrm{EPO}}(t - T_P) \tag{38}$$

The probability density functions tested for reticulocyte lifespan variation included gamma $\ell_n(\tau)$ Eq. (12), Dornhorst $\ell_D(\tau)$ Eq. (17), and lognormal $\ell_{\log}(\tau)$ Eq. (31) distributions and these models allowed estimating the mean and standard deviation for the reticulocyte population. When

$\ell_D(\tau)$ was used for, the reticulocyte lifespan distribution, the convolution operator in Eq. (37) was calculated according to Eqs. (18) and (19). The reticulocyte data were simultaneously fitted with fixed PK parameters. In response to rHuEPO or severe anemia (erythropoietic stress), reticulocytes are released prematurely from the bone marrow and mature in the circulation (24). This increased portion of younger reticulocytes requires the parameters λ and T_R to vary with dose. The mean (T_{RET}) and standard deviation (SD_{RET}) for the reticulocyte lifespan distribution were calculated from Eq. (2) as secondary parameters

$$T_{\mathrm{RET}} = \frac{1}{\lambda}\left(1 - e^{-\lambda T_R}\right) \quad \text{and} \quad SD^2_{\mathrm{RET}} = \frac{1}{\lambda^2}\left(1 - 2\lambda T_R e^{-\lambda T_R} - e^{-2\lambda T_R}\right) \tag{39}$$

For the gamma distribution p.d.f. $\ell_n(\tau)$, Eq. (37) was calculated based on Eqs. (13)–(15). The $n = 40$ was assigned throughout the fittings and the τ_0 was estimated in a dose-dependent manner. The T_{RET} and SD_{RET} for the reticulocyte lifespan distribution were obtained from n and τ_0 according to Eq. (26). The lognormal distribution $\ell_{\log}(\tau)$ was approximated by the histogram Eq. (21) and the convolution in Eq. (37) was solved by Eqs. (22)–(23). The parameters m and σ were allowed to vary with dose and these estimated parameters were subsequently used to compute the distribution parameters for the reticulocyte pool as follows:

$$T_{\mathrm{RET}} = e^{(m+\sigma^2/2)} \quad \text{and} \quad SD^2_{\mathrm{RET}} = e^{(2m+2\sigma^2)} - e^{(2m+\sigma^2)} \tag{40}$$

The number of bins for the histogram was $n = 100$ and $\Delta\tau = 3.5\,\mathrm{h}$. To compare the lifespan distribution models with the fixed lifespan model for describing the responses, this data set was also reanalyzed using the fixed lifespan distribution (i.e., $SD_{\mathrm{RET}} = 0$) with a dose-dependent mean lifespan of reticulocyte (T_{RET}) to make the estimated parameters and goodness-of-fit criteria comparable with those from other models.

The models were allowed to estimate the endogenous precursor production rate $k_{\mathrm{in}R}$. The baseline reticulocyte counts (R_0) were calculated as a secondary parameter by rearranging Eq. (30). In addition, since erythropoietin is present endogenously, the baseline of the cell population needed to take into consideration the predose level of erythropoietin (C_0) and yielded

$$R_0 = k_{\mathrm{in}R} \cdot T_{\mathrm{RET}} \cdot \left(1 + \frac{S_{\max} \cdot C_0}{SC_{50} + C_0}\right) \tag{41}$$

The baseline of endogenous erythropoietin (C_0) was fixed at the value of 13.55 mIU/ml obtained by averaging the pre-dose values from all doses. The estimations were performed by ADAPT II (21) using the maximum

likelihood estimator with the variance model Eq. (32) where Y denoted the model predicted reticulocyte counts and a and b were variance parameters. ADAPT II subroutines used to calculate $C_{\mathrm{EPO}}(t)$ and reticulocyte response R for all lifespan distributions discussed above are shown in Appendix D.

RESULTS

Simulations

The effects of dose on the response curve for a cell population with a continuous lifespan distribution are shown in Fig. 3. Contrary to responses generated for a population with the point lifespan distribution, the responses lack sharp peaks and the peak times depend on dose. With increasing doses the peaks shift to later times and become sharper. Also, the peak values increase with increasing doses to approximate the peak values for the fixed lifespan responses. Since these approach the limiting value $R_0 \cdot (1 + S_{\max})$ for large doses, we can conclude that the same limit is achieved by the responses for cell populations with continuous lifespan distribution if doses become very large.

The peak time for the response curve for the basic LIDR model well correlates with the peak time for the lifespan distribution as shown in Fig. 4. For the gamma distribution the peaks occur at $T - \tau_0$ where T is the distribution mean. Consequently, increase in the population mean lifespan with conserved SD results in delay of the peak response. Additionally, the response peak value decreases and the peak plateaus. This behavior was observed for the cell populations with the point lifespan distribution (6). Fig. 5 shows the response vs. time profiles for the cell populations with the same mean lifespan but varied SD. The sharpest response corresponds to the point distribution ($SD = 0$). With increased SD, the peak becomes shallower and the peak value decreases, indicating that the increased variability in lifespan distribution results in dispersion of the response. However, the change in SD does not alter the peak time of the response but it remains the same.

In the presence of a precursor pool the responses for the basic LIDR model are delayed. As shown in Fig. 6 the lag times for the response vs. time curves correlate with the mean lifespan for the precursor pool (T_M). The response profiles are shifted by the lag time and their shapes are conserved. This is because the major determinants of the response T_R, SD_R, and $k_{\mathrm{in}R}$ were the same, contrary to analogous determinants for the precursor pool M. Both T_M and M_0 are varying which results in different baseline values as seen in Fig. 6. Similar behavior of the responses for the

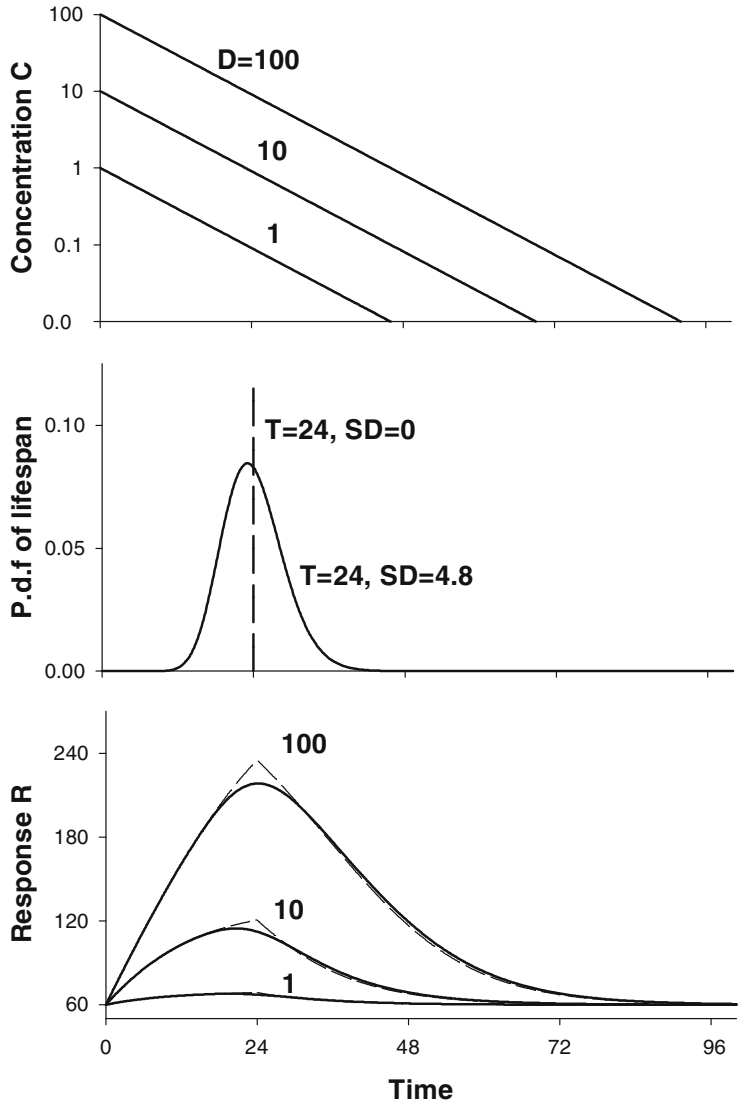

Fig. 3. Effect of dose on the response vs. time curve. The responses for the basic LIDR models were simulated (lower panel). The monoexponential pharmacokinetic function was used with $k_{el} = 0.1, V = 1$ and the indicated doses (upper panel). The cell lifespan distribution was described by the gamma p.d.f. Eq. (12) with $\tau_0 = 0.96$ and $n = 25$ that corresponded to the mean lifespan $T = 24$ and $SD = 4.8$ (middle panel). The PD parameters used for simulations were $S_{max} = 4$, $SC_{50} = 10$, and $R_0 = 60$. The cell production rate $k_{in R}$ was calculated from Eq. (30). The broken line indicates the response for the population with a point lifespan distribution ($T = 24$, $SD = 0$).

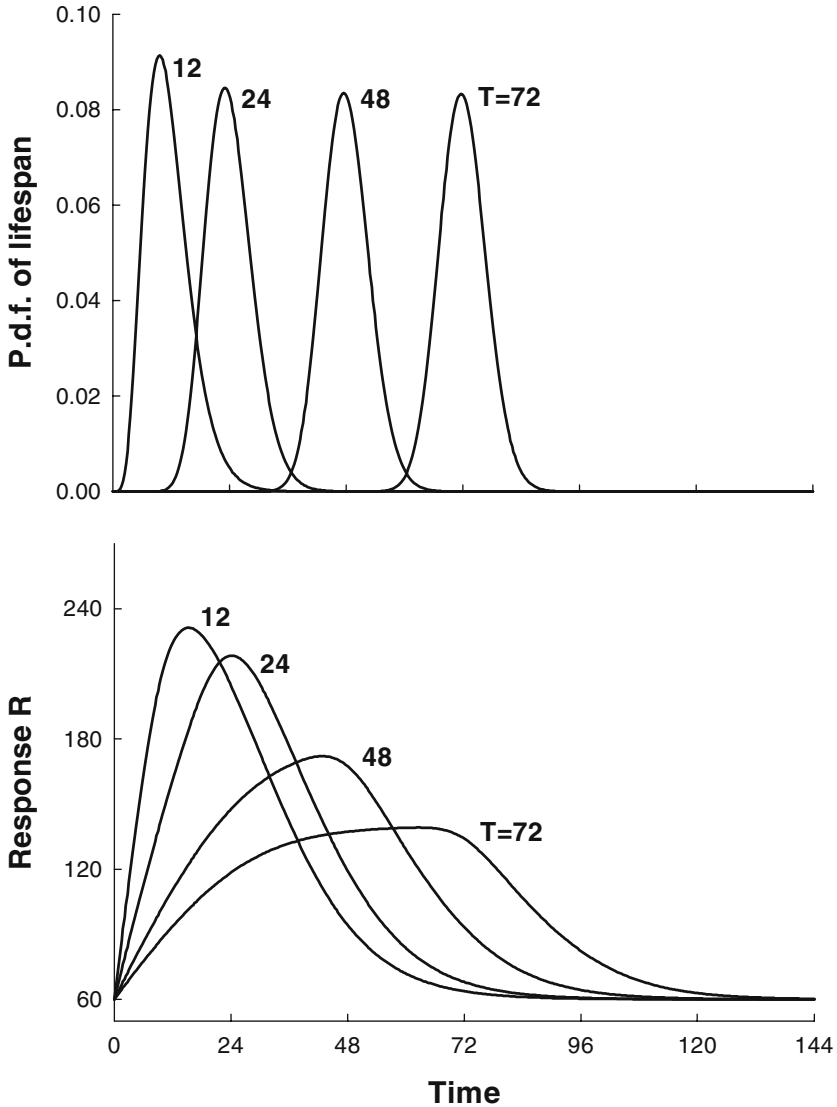

Fig. 4. Effect of the mean lifespan on the response vs. time curves for the basic LIDR model. The responses after a single dose of 100 for four cell populations with the gamma distributions of lifespans with the means of 12, 24, 48 and 72 and *SD* of 4.8 (upper panel) were simulated (lower panel). The remaining values for the PK/PD parameters were as in Fig. 3.

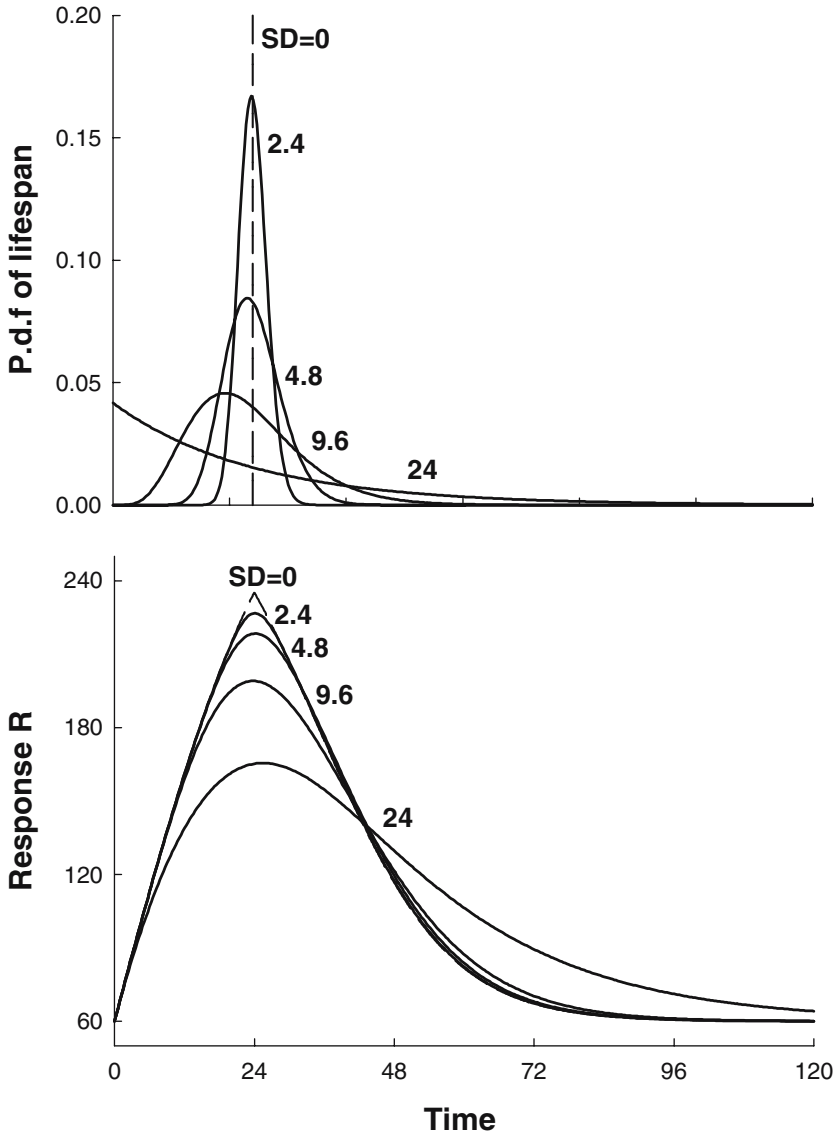

Fig. 5. Effect of the *SD* on the response vs. time curves for the basic LIDR model. The responses after a single dose of 100 for cell populations with gamma distributions of lifespan with the mean of 24 and *SD* of 2.4, 4.8, 9.6, and 24 (upper panel) were simulated (lower panel). The remaining values for the PK/PD parameters were as in Fig. 3. The broken line indicates the response for the population with a point lifespan distribution.

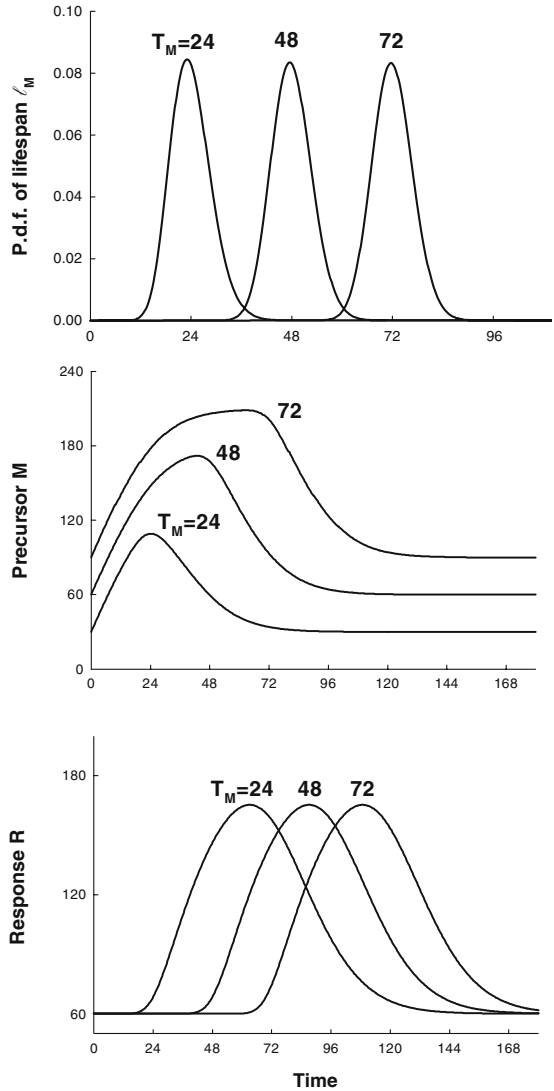

Fig. 6. Effect of the mean precursor lifespan on the response vs. time curves for the basic LIDR model with a precursor. The responses R after a single dose of 100 for precursor cell populations M with gamma distributions of lifespan with means of 24, 48 and 72 and SD_M of 4.8 (upper panel) were simulated for the precursor pool M (middle panel) and the central pool R (lower panel). The mean lifespan for the central pool was $T_R = 48$ and $SD_R = 9.6$. The production rate $k_{\text{in}R}$ was calculated from Eq. (30) and was used as $k_{\text{in}0}$ in Eq. (9) and (11) which were applied to determine M. The remaining values for the PK/PD parameters were as in Fig. 3.

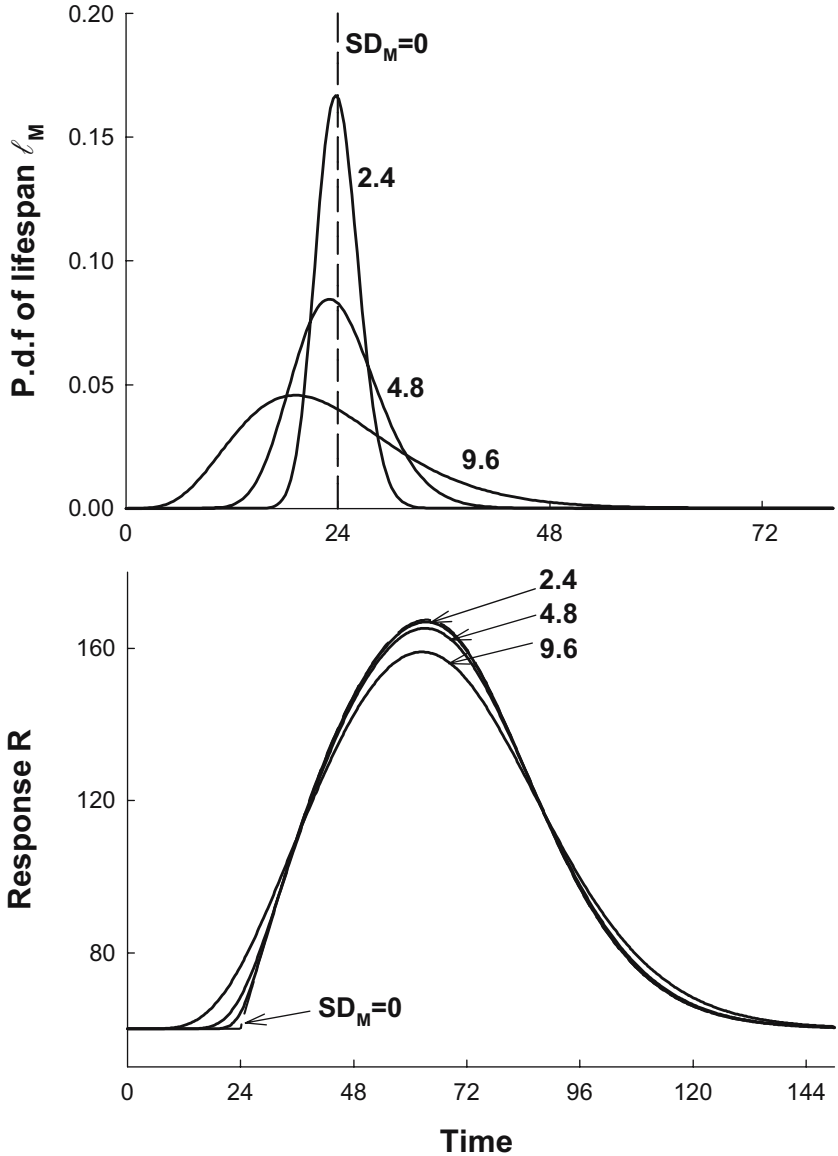

Fig. 7. Effect of the SD of the precursor lifespan distribution on the response vs. time curves for the basic LIDR model with a precursor. The responses R after a single dose of 100 for precursor cell populations M with gamma distributions of lifespan with the mean of 24 and SD_M of 2.4, 4.8, and 9.6 (upper panel) were simulated (lower panel). The remaining values for the PK/PD parameters were as in Fig. 6. The broken line indicates the response for the population with point lifespan distribution.

precursor and central pools were observed for the point lifespan distributions (6).

The effect of varying SD_M in the precursor lifespan distribution on the response R is shown in Fig. 7. Two-fold change in SD_M results in little change of the response curve that approximates the response vs. time profile corresponding to the point precursor lifespan distribution. The peak time remains the same since the mean lifespan values for the precursor and central pools are the same.

Estimability of PD Parameters in the Basic LIDR Model

The identifiability of basic LIDR model Eq. (28) was tested on a simulated 2 dose and placebo response data set. One hundred data sets with normally distributed noise having a coefficient of variation of about 20% were fitted by the same equation and parameter estimates were recorded. The lognormal distribution of lifespans (Eq. 31) was assumed and was approximated by p.d.f. Eq. (21). The minimization did not converge in 8 cases due to numerical problems with solving differential equations. The estimated σ values for 5 data sets were greater than 3.0 (10-fold higher than the true value), and the PD parameter estimates were excluded from further analysis. The histograms of frequency distributions of the estimates are shown in Figs. 8 and 9. The largest dispersion about the true value was observed for σ and SC_{50} indicating the low precision of their estimates. The $RMSPE$ for σ was 215% and for SC_{50} it was 93%, whereas $RMSPE$ for the estimates of remaining PD parameters were below 30% (see Table I). The low precision of σ propagated on the variability of SD_{hist} but not on T_{hist} and was lower than the variability of σ. Both σ and SC_{50} were distinctly biased with MPE higher than 30%. No bias was detected for the estimates of the remaining PD parameters including calculated T_{hist} and SD_{hist}.

Stimulation of Reticulocyte Production by rHuEPO

The biexponential function with a lag time (Eq. 31) was used to fit the rHuEPO serum concentration versus time data. This empirical function was fitted to the data and PK parameters were estimated for each dose level. Such an approach was taken to avoid developing a complex PK model that might not satisfactorily describe the data and contribute to improper identification of the PD model parameters. The PK parameters were fixed for the PD data analysis. Their estimated values are presented in Table II.

The fixed lifespan IDR model (6) was modified so that the Dornhorst distribution $\ell_D(\tau)$ Eq. (17), gamma distribution $\ell_n(\tau)$ Eq. (12), and

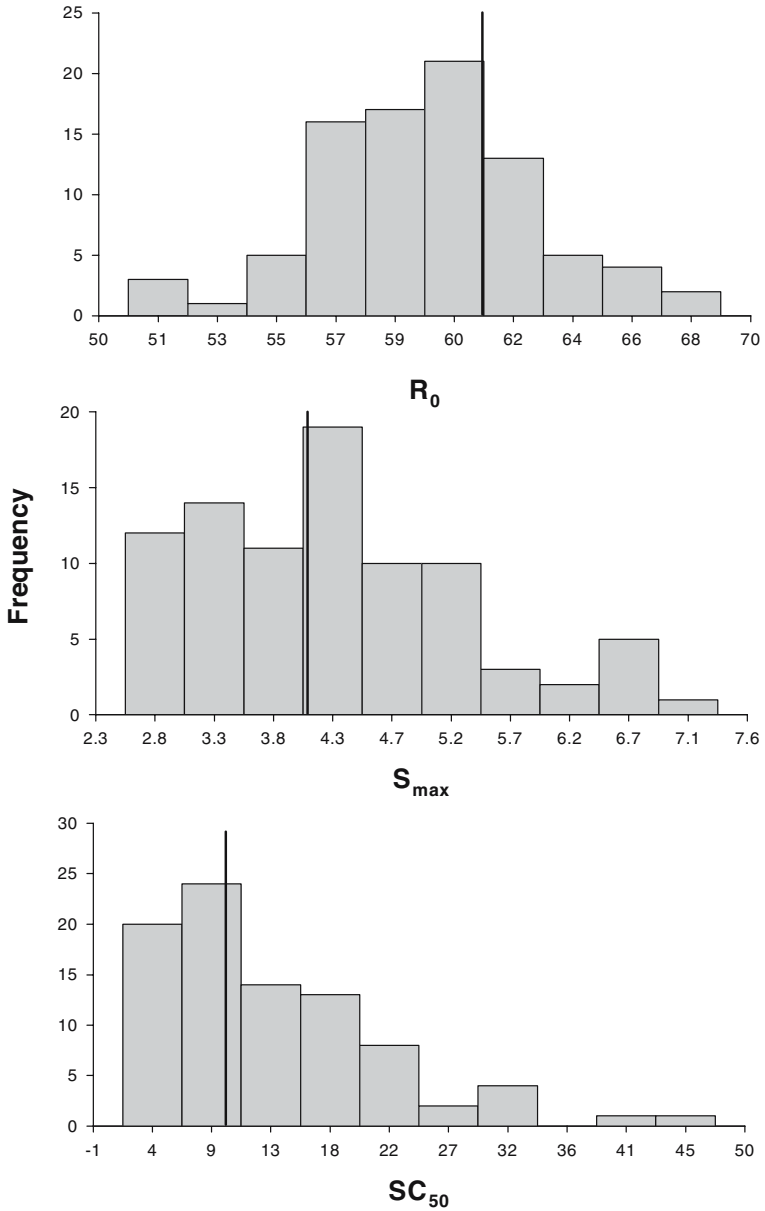

Fig. 8. Histograms of frequency distributions of estimates of $R_0, S_{\max}$, and SC_{50}. One hundred responses described in Fig. 2 were fitted by Eq. (28) and the values of the PD parameters were recorded if the estimation was successful. The vertical lines denote the true parameter values listed in Table I.

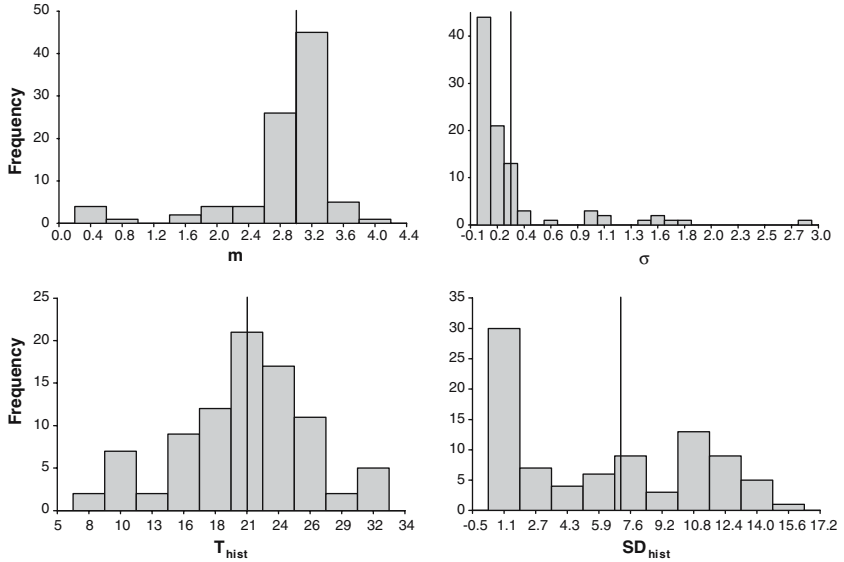

Fig. 9. Histograms of frequency distributions of estimates of the lifespan parameters in Eq. (28). The parameter estimates m and σ were obtained as described in Fig. 8. T_{hist} and SD_{hist} were secondary parameters calculated from Eq. (24). The vertical lines denote the true parameter values listed in Table I.

Table I. The Bias and Precision of Estimates of PD Parameters for the Basic LIDR Model with the Lognormal Lifespan Distribution

Parameter	True value	Mean	SD	MPE	RMSPE
R_0	60	59.7	3.5	−0.5	5.7
$S_{\max}$	4	4.3	1.1	6.5	27.8
SC_{50}	10	13.1	8.9	31.1	93.3
m	3	2.9	0.5	−2.2	16.7
σ	0.3	0.44	0.63	48.0	215
T_{hist} [a]	21	21.0	5.6	−0.2	26.3
SD_{hist} [a]	6.4	6.1	4.9	−5.7	75.5

The number of successful minimizations was 87 out of 100 analyzed data sets.
[a] secondary parameter
MPE – mean percent predictive error.
RMSPE – the root mean squared prediction percent error.

lognormal distribution $\ell_{\log}(\tau)$ Eq. (31) were used to describe the p.d.f. for the reticulocyte lifespan and the convolution operator in Eq. (37) was calculated according to Eqs. (18)–(19), Eqs. (13)–(15), and Eqs. (22)–(23), respectively. Our objective was to determine if any of these distribu-

Table II. The Estimated Values of PK Parameters for rHuEPO

	Dose (IU/kg)			
Parameter	450	900	1350	1800
C_0, IU/l	13.55[a]	13.55[a]	13.55[a]	13.55[a]
C_1, IU/l	932 (15)	2142 (16)	3291 (19)	5427 (14)
C_2, IU/l	200.7 (41)	292.4 (55)	490.5 (42)	345.3 (94)
k_1, h^{-1}	0.135 (25)	0.073 (22)	0.081 (25)	0.045 (17)
k_2, h^{-1}	0.031 (17)	0.022 (20)	0.022 (15)	0.017 (30)
t_{lag}, h	39.0 (11)	38.4 (14)	41.3 (15)	42.2 (12)

The parameters were obtained from fitting Eq. (35) to the data from (20). The numbers in parenthesis denote CV%.
[a] parameter was fixed in the fitting procedure.

tions was better suited for the reticulocyte data than the point distribution used in the fixed lifespan model. We allowed the p.d.f. parameters to be dose-dependent. The remaining PD parameters were same across all doses. The reticulocyte baselines, T_{RET}, and SD_{RET} were calculated as secondary parameters. The estimated values of PD parameters are shown in Table III. The gamma and lognormal distribution LIDR models performed similarly to the fixed lifespan model both in terms of goodness of fits and the estimated values of the PD parameters. The Dornhorst distribution LIDR model resulted in the best fitting measured by the value of the objective function (OBJF) (see Fig. 10). For this model the estimates of the reticulocyte random destruction rate (λ) were highly variable and resulted in values ranging from 0.0001 to 0.005 h^{-1}. The estimates of the reticulocyte senescent lifespan T_R were in the range 7.1 to 7.9 days, resulting in the mean reticulocyte lifespan T_{RET} of 5.0 to 7.4 days, and SD_{RET} of 0.7 to 2.8 days. Although T_{RET} and SD_{RET} were calculated from T_R and λ, the imprecision in λ estimates did not propagate on variability of T_{RET} and SD_{RET} values (CV% ranged 6–10%). The estimates of drug related parameters S_{max} and SC_{50} were 5.7 and 206 IU/L, respectively. Since the absolute values of reticulocyte counts were not available, the reported k_{in} was expressed as percent increase per hour. All LIDR models were inferior to the fixed lifespan model based on Akaike Information Criterion (25) mostly due to an increase in number of lifespan distribution PD parameters that did not improve the fittings. However the AIC values were not noticeable different for any of these models (range 86–93).

Table III. The Estimated Values of PD Parameters and Goodness-of-fit Criteria from Four Different LIDR Models for the Stimulation of Reticulocyte Production by rHuEPO

Model	Fixed life-span		Dornhorst		Gamma Distribution		Lognormal Distribution	
AIC		86.01		87.56		88.34		92.86
OBJF		33.01		29.78		34.17		32.43
Parameters estimated	S_{max}	4.1 (16)	S_{max}	5.7 (13)	S_{max}	4.4 (18)	S_{max}	4.5 (16)
	SC_{50}	345.9 (57)	SC_{50}	205.5 (60)	SC_{50}	350.2 (78)	SC_{50}	385.1 (59)
	T_P	56.1 (10)	T_P	58.9 (9)	T_P	57.5 (10)	T_P	57.1 (9)
	$T_{RET,450}$	168.5 (7)	$T_{R,450}$	170.6 (8)	$\tau_{0,450}$	4.1 (10)	$m_{,450}$	5.1 (2)
	$T_{RET,900}$	165.8 (7)	$T_{R,900}$	174.3 (9)	$\tau_{0,900}$	4.0 (9)	$m_{,900}$	5.1 (2)
	$T_{RET,1350}$	175.6 (6)	$T_{R,1350}$	189.2 (8)	$\tau_{0,1350}$	4.3 (9)	$m_{,1350}$	5.2 (2)
	$T_{RET,1800}$	190.0 (6)	$T_{R,1800}$	180.1 (6)	$\tau_{0,1800}$	4.6 (8)	$m_{,1800}$	5.2 (2)
			$\lambda_{,450}$	0.0028[a]	k_{inR}	0.0079 (10)	$\sigma_{,450}$	0.1 (186)
			$\lambda_{,900}$	0.0047[a]			$\sigma_{,900}$	0.3 (64)
			$\lambda_{,1350}$	0.0045[a]			$\sigma_{,1350}$	0.1 (78)
			$\lambda_{,1800}$	0.0001[a]			$\sigma_{,1800}$	0.02[a]
Secondary parameters	k_{inR}	0.0077 (9)	k_{inR}	0.0064 (17)			k_{inR}	0.0077 (10)
	$R_{0,450}$	1.50 (4)	$R_{0,450}$	1.47 (5)	$R_{0,450}$	1.49 (5)	$R_{0,450}$	1.49 (5)
	$R_{0,900}$	1.47 (5)	$R_{0,900}$	1.50 (5)	$R_{0,900}$	1.47 (5)	$R_{0,900}$	1.46 (5)
	$R_{0,1350}$	1.56 (5)	$R_{0,1350}$	1.63 (5)	$R_{0,1350}$	1.57 (5)	$R_{0,1350}$	1.56 (5)
	$R_{0,1800}$	1.69 (5)	$R_{0,1800}$	1.55 (6)	$R_{0,1800}$	1.70 (5)	$R_{0,1800}$	1.69 (6)
			$T_{RET,450}$	135.7 (6)	$T_{RET,450}$	162.3 (10)	$T_{RET,450}$	167.3 (9)
			$SD_{RET,450}$	53.9 (10)	$SD_{RET,450}$	25.7 (10)	$SD_{RET,450}$	16.9 (185)
			$T_{RET,900}$	119.3 (6)	$T_{RET,900}$	160.3 (9)	$T_{RET,900}$	163.0 (9)
			$SD_{RET,900}$	61.5 (10)	$SD_{RET,900}$	25.3 (9)	$SD_{RET,900}$	44.6 (58)

Table III. Continued

Model	Fixed life-span	Dornhorst		Gamma Distribution		Lognormal Distribution	
		$T_{\mathrm{RET},1350}$	127.7 (5)	$T_{\mathrm{RET},1350}$	171.2 (9)	$T_{\mathrm{RET},1350}$	175.1 (8)
		$SD_{\mathrm{RET},1350}$	67.0 (9)	$SD_{\mathrm{RET},1350}$	27.1 (9)	$SD_{\mathrm{RET},1350}$	20.3 (77)
		$T_{\mathrm{RET},1800}$	177.8 (6)	$T_{\mathrm{RET},1800}$	185.3 (8)	$T_{\mathrm{RET},1800}$	189.2 (7)
		$SD_{\mathrm{RET},1800}$	16.2 (10)	$SD_{\mathrm{RET},1800}$	29.3 (8)	$SD_{\mathrm{RET},1800}$	3.9[a]

The numbers in parenthesis denote CV%.
[a] CV% greater than 1000%.
Units: SC_{50} (IU/l), T_P (h), T_R (h), $k_{\mathrm{in}R}$ (%/h), R_0 (%), λ (h^{-1}), m(h), σ(h), T_{RET} (h), SD_{RET} (h), τ_0 (h).
Abbreviations: AIC (Akaike Information Criterion), OBJF (objective function).

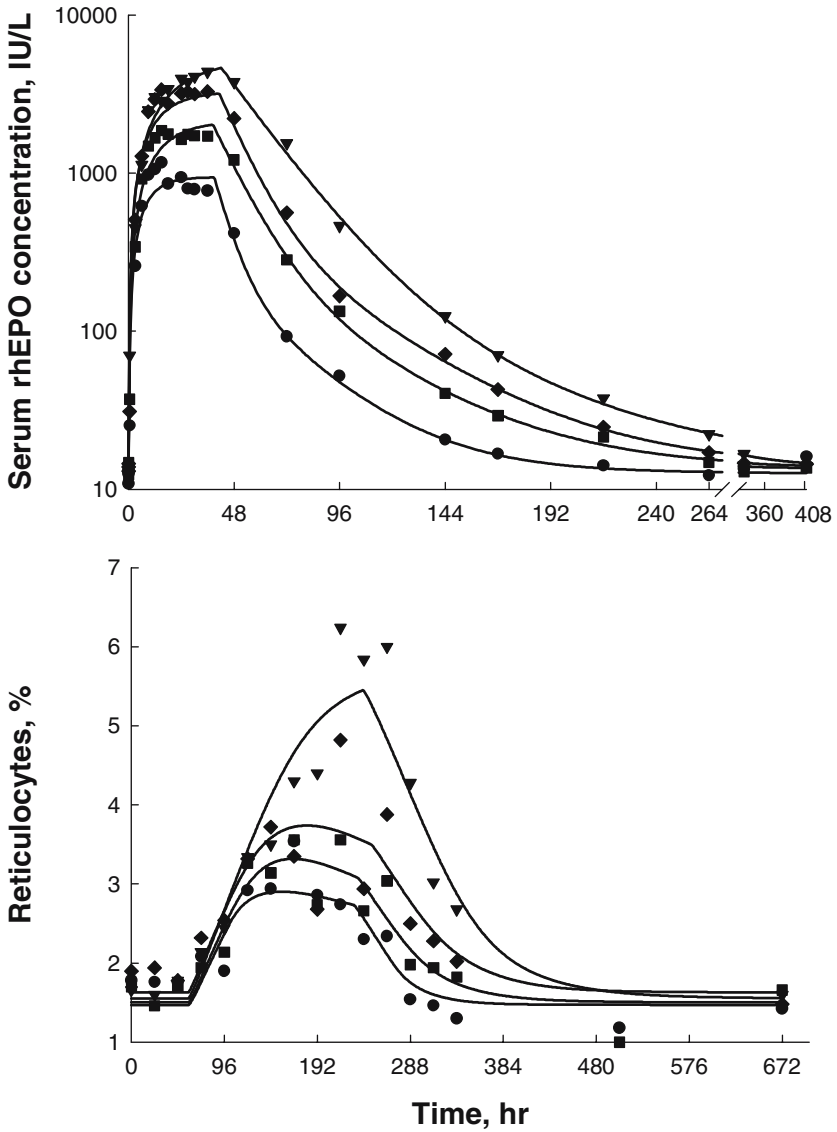

Fig. 10. Fitting of serum rHuEPO concentrations (upper panel) using Eq. (35) and reticulocyte counts versus time (lower panel) using Eq. (37) after subcutaneous administration of rHuEPO doses of (●) 450, (■) 900, (♦) 1350, and (▼) 1800 IU/kg. The values of fitted parameters are presented in Tables II and III. Original data were obtained from (20).

DISCUSSION

The PD models presented are a natural extension of previous models describing cell turnover affected by a therapeutic agent but restricted by the assumption of a single lifespan for all cells in the population (6). We derived all equations necessary to account for a continuous distribution of cell lifespans preserving the same paradigm that cell loss is determined by the expiration of cell lifespans. The subsequent mathematical formalism replaced the delay operator with the convolution integral and the numerical problem of calculating it arose. We presented several p.d.f. that were particularly useful for that purpose including a calculation of the convolution operator for a histogram that can approximate any arbitrary lifespan p.d.f..

The properties of the gamma p.d.f. are very convenient for description of the continuous lifespan distribution. If the gamma function is used, then the convolution integral describing the cell elimination rate can be calculated by solving a system of ordinary differential equations that have the structure of the transduction model (26). Transit compartments for modeling the delay between the site of drug action and measurable response have been used to describe platelet (1) and leukocyte (2) kinetics. In our model they are not present, since they are only a means of numerical calculation of the convolution integral. If computer software allows, then other typical p.d.f. (e.g., normal distribution) can be used to describe cell lifespan distributions. However, available programs for PK/PD analysis do not include calculation of the convolution integral and the techniques presented in this report merely circumvent this computational obstacle.

Simulations were performed using the gamma distribution p.d.f. to assess the role of the key PD parameters in controlling the shape of the response vs. time curve. Another objective was to determine the differences between the proposed model and the fixed lifespan model introduced previously (6). Unlike the previous observation that the peak time of the response was dose-independent, it was found that the maximum response occurs later with increasing doses. As expected, these models coincide if the standard deviation of lifespan distribution becomes very small. Increase in the SD results in attenuation of the response curve: the peak diminishes and the curve flattens. However, the changes in SD for either precursor or central pools do not change the time of the maximum responses. The dependence of the response on the mean lifespan of the central as well as precursor cell pools is analogous to the fixed lifespan models. Accordingly, the mean lifespans can be easily identified from the peak and lag times of the response curve. However, one can expect difficulties in precisely resolving the SD parameter for the central pool. Based

on our simulations, the small change in SD of precursor lifespan distribution may not be significant in controlling the response profiles, suggesting that the SD for the precursor might not be identified from the central pool response unless the precursor population was also measured.

Our expectation of problems with identifiability of the SD from the LIDR data was confirmed by the results of the LIDR model identifiability study where we attempted to estimate PD parameters from a data generated with their known values. The SD was highly variable as well as the estimates of SC_{50}. The estimates of remaining PD parameters (including the mean lifespan T) were neither biased nor imprecise. The problems with accurate and precise resolution of the EC_{50} parameter of the IDR models have been reported previously (27,28). The reason for poor estimability of SD is the limited information about this parameter contained in the response vs. time data. This is an inherent problem even for cell survival studies designed to obtain T and SD values only (29). A suggested approach to rectify this problem is to apply the LIDR model with a fixed lifespan and compare it with the LIDR model containing SD. The metrics of model performance (e.g., Akaike Information Criterion (25)) can be used to make a selection. Ideally, one can improve the precision of SD estimates by adding cell survival data to the experimental design. Such an approach has been successful in PK/PD modeling of drug effects on platelet lifespan (1).

Literature data were used to exemplify applications of LIDR model to reticulocytes stimulated by rHuEPO (20). The estimates of PK parameters for rHuEPO serum concentrations did not differ from those previously reported (6) since both the data and the PK model were the same. The PD data were refitted with the LIDR models that applied all lifespan p.d.f. presented in this report. We aimed at testing if any of the p.d.f. resulted in a better fitting of the data. None of the models yielded noticeable improvement of the fittings measured by the objective function value than the fixed lifespan models. Also, the AIC values were comparable across all models meaning that the slight improvement in fittings was at expense of an increased number of estimated parameters. Therefore we conclude that for the tested data the LIDR models performed equally well as the fixed lifespan model. The estimated values of PD were consistent with the analogous parameters reported previously for the same data set (6). The SC_{50} remained inside the 95% confidence intervals. The 4-fold increase in the S_{max} value might be caused by the lack of the cell magnifying factor η in our PD model. Reticulocyte data exhibited a rebound in later times, whereas our model necessitated that responses return to the baseline. Consequently, the terminal parts of the data were over-predicted. The tolerance phenomenon in reticulocyte counts has been reported in the

literature. Possible mechanisms include a negative delayed feedback from the circulation to the production of progenitor cells (30) or depletion of early progenitor cell pool (31). The advantage of the LIDR models over the fixed lifespan model was additional information gained on variability of the lifespan of the circulating cells. Since there is limited information in the literature reporting SD of lifespan distributions for reticulocytes, assessment of accuracy of our estimates is difficult.

The presented cases of data analysis demonstrate the applicability of the continuous cell lifespan distribution approach in modeling cell turnover affected by a therapeutic agent. These models are more flexible than the fixed lifespan LIDR models, however the standard deviation of the lifespan distribution might not be estimated as precisely as the mean. The drug efficacy ($S_{\max}$) and potency (SC_{50}) can be accurately identified. The use of the convolution operator generalizes the transit compartment approach to modeling signal transduction. Further development of computational tools is necessary to explore use of various cell lifespan distributions in controlling cell responses.

APPENDIX A

Derivation of Eq. (4)

By definition, for a small time increment Δt,

$$k_{\text{in}}(t)\Delta t = \text{ No. cells that entered the population between times } t \text{ and } t + \Delta t \tag{A1}$$

$$k_{\text{out}}(t)\Delta t = \text{ No. cells that exited the population between times } t \text{ and } t + \Delta t \tag{A2}$$

If the distribution of lifespans for the cell population is known, then the cell loss rate $k_{\text{out}}(t)$ is uniquely determined by the production rate $k_{\text{in}}(t)$ and the p.d.f. for the lifespan distribution $\ell(\tau)$. To derive this relationship, notice that for a small lifespan increment $\Delta\tau$

$$k_{\text{in}}(t)\Delta t\ell(\tau)\Delta\tau = \text{ No. cells that entered the population between times } t \text{ and } t + \Delta t \text{ and have lifespans between } \tau \text{ and } \tau + \Delta\tau \tag{A3}$$

Suppose that all cells that enter the population have age 0; then this cohort of cells $k_{\text{in}}(t)\Delta t\ell(\tau)\Delta\tau$ will exit the population between the times

$t + \tau$ and $t + \tau + \Delta t + \Delta\tau$. Consequently, it will contribute to the number $k_{\text{out}}(t + \tau)(\Delta t + \Delta\tau)$. By the same token, the number of cells that entered the population at $t - \tau, k_{\text{in}}(t - \tau)\Delta t\ell(\tau)\Delta\tau$ will contribute to the number of cells that exited the population at time $t, k_{\text{out}}(t)(\Delta t + \Delta\tau)$. If τ is not continuous but discrete, $\tau = i\Delta\tau,\ i = 0, 1, \ldots$, then the contributions of cells of lifespans $i\Delta\tau$ entering the population will be included to $k_{\text{out}}(t)(\Delta t + \Delta\tau)$ when the entry times are $t - i\Delta\tau, \quad i = 0, 1, \ldots$. Therefore

$$k_{out}(t)(\Delta t + \Delta\tau) = \sum_{i=0}^{\infty} k_{\text{in}}(t - i\Delta\tau)\Delta t\ell(i\Delta\tau)\Delta\tau \tag{A4}$$

Letting $\Delta\tau \to 0$, the sum in Eq. (A4) becomes the integral and

$$k_{\text{out}}(t)\Delta t = \int_0^{\infty} k_{\text{in}}(t - \tau)\Delta t\ell(\tau)d\tau \tag{A5}$$

After canceling out of Δt from both sides of Eq. (A5) one can derive Eq. (4).

APPENDIX B

Baseline Equation

If the production rate $k_{\text{in}}(t) \equiv k_{\text{in0}}$ is constant, then the right hand side of Eq. (5) is 0, and there is an infinite number of solutions. To select the baseline solution N_0 one can state an additional requirement that in the absence of cell production the cell number must decline to 0 for large times. This can be written as

$$\frac{dN}{dt} = \theta(-t)k_{in0} - k_{in0}\theta(-t) * \ell(t) \tag{B1}$$

and

$$N(t) \to 0 \text{ as } t \to \infty \tag{B2}$$

The solution of Eq. (B1) for $t \geq 0$ is of the form

$$N(t) = N_0 - k_{\text{in0}}t\int_t^{\infty} \ell(\tau)d\tau - k_{\text{in0}}\int_0^t \tau\ell(\tau)d\tau \tag{B3}$$

Assuming that the first moment of $\ell(\tau)$ exists (see Eq. 4), the condition Eq. (B2) is satisfied only if

$$N_0 = k_{\text{in}0} \int_0^\infty \tau \ell(\tau) d\tau \tag{B4}$$

Eq. (B4) expresses the baseline value.

APPENDIX C

Calculation of the Convolution Integrals

The basic relationship for all of subsequent derivations is

$$\frac{d}{dt}\left(k_{\text{in}} * \ell\right)(t) = k_{\text{in}}(t) \cdot \ell(0) + k_{\text{in}} * \frac{d\ell}{dt}(t) \tag{C1}$$

If $\ell_n(t)$ is the gamma function in Eq. (12), then for $i > 1$

$$\frac{d(k_{\text{in}} * \ell_i)}{dt} = \frac{1}{\tau_0} k_{\text{in}} * \ell_{i-1} - \frac{1}{\tau_0} k_{\text{in}} * \ell_i \quad \text{and } k_{\text{in}} * \ell_i(0) = k_{\text{in}0} \tag{C2}$$

and for $i = 1$

$$\frac{d(k_{\text{in}} * \ell_1)}{dt} = \frac{1}{\tau_0} k_{\text{in}}(t) - \frac{1}{\tau_0} k_{\text{in}} * \ell_1 \text{ and } k_{\text{in}} * \ell_1(0) = k_{\text{in}0} \tag{C3}$$

If X_i denotes the solution of Eq. (14) or (15), then

$$X_i = k_{\text{in}} * \ell_i \tag{C4}$$

and Eq. (13) follows. If $\ell_D(t)$ is described by Eq. (17), then

$$k_{\text{in}} * \ell_D(t) = k_{\text{in}}(t - \tau_R) e^{-\lambda \tau_R} + \lambda k_{\text{in}} * (\theta(\tau_R - t) e^{-\lambda t}) \tag{C5}$$

If one defines X as

$$X = k_{\text{in}} * (\theta(\tau_R - t) e^{-\lambda t}) \tag{C6}$$

then the differentiation of X results in Eq. (19), since

$$\frac{d}{dt}\left(\theta(\tau_R - t) e^{-\lambda t}\right) = \delta(\tau_R - t) e^{-\lambda t} - \lambda \theta(\tau_R - t) e^{-\lambda t} \tag{C7}$$

and direct integration shows that

$$k_{\text{in}} * (\theta(\tau_R - t)e^{-\lambda t})(0) = \frac{1}{\lambda}\left(1 - e^{-\lambda\tau_R}\right) \tag{C8}$$

To derive Eq. (23) one can integrate its both sides. The direct integration results in

$$\int_0^\infty k_{\text{in}}(t-\tau)\ell_{\text{hist}}(\tau)d\tau = \sum_{i=1}^{n} a_i \int_{\tau_i}^{\tau_{i+1}} k_{\text{in}}(t-\tau)d\tau \tag{C9}$$

For $i = 1, 2, \ldots, n+1$ let us define

$$X_i = \int_0^{\tau_i} k_{\text{in}}(t-\tau)d\tau \tag{C10}$$

Then Eq. (C9) can be written as

$$k_{\text{in}} * \ell_{\text{hist}}(t) = \sum_{i=1}^{n} a_i (X_{i+1} - X_i) \tag{C11}$$

Evaluation of Eq. (C10) at $t = 0$ yields

$$X_i(0) = k_{\text{in}0}\tau_i \tag{C12}$$

Since

$$\int_0^{\tau_i} k_{\text{in}}(t-\tau)d\tau = \int_{t-\tau_i}^{t} k_{\text{in}}(\tau)d\tau \tag{C13}$$

from Eq. (C10) it follows that

$$\frac{dX_i}{dt} = k_{in}(t) - k_{\text{in}}(t-\tau_i) \tag{C14}$$

Eqs. (C11) and (C14) are exact versions of Eqs. (22) and (23).

APPENDIX D

ADAPT II Subroutines for Modeling the Reticulocyte Response

All codes are presented to model a single rHuEPO dose (450 IU/kg) reticulocyte response. Straightforward adjustments are necessary to account for modeling of multiple dose responses.

Pharmacokinetic Function Describing rHuEPO Serum Concentrations

The parameters C_1, C_2, k_1, and k_2 were estimated from the PK data and subsequently fixed at their estimated values to analyze the PD data.

```
Function Cepo (t)
Implicit none
Include 'globals.inc'
Include 'model.inc'
Real*8 Cepo,Ct,Cepo0,T,C1,C2,k1,k2,tlag
Cepo0=13.55
C1=932
C2=200.7
k1=0.135
k2=0.031
tlag=39.0
If =(T.GT.0) Then
   If=(tlag.GE.T) Then
     Ct=C1*(1-EXP(-k1*T))
   Endif
   If (tlag.LT.T) Then
     Ct=C1*(EXP(-k1*(T-tlag))-EXP(-k1*T))
     +C2*(EXP(-k2*(T-tlag))-
       EXP(-k1*(T-tlag)))
   Endif
Else
     Ct=0
   Endif
     Cepo=Cepo0 + Ct
Return
End
```

Reticulocyte Response Described by the Fixed Lifespan IDR Model

```
Subroutine DIFFEQ(T,X,XP)
Implicit None
Include 'globals.inc'
Include 'model.inc'
Real*8 T,X(MaxNDE),XP(MaxNDE)
Real*8 kin,R0,Smax,SC50,Tr,Tp,lambda,HCt0,HCtP,
Real*8 HCtR,Cepo
Smax=P(1)
```

```
SC50=P(2)
Tp=P(3)
Tr=P(4)
kin=P(5)
HCt0=1+Smax*Cepo(0.0)/(SC50+Cepo(0.0))
HCtP=1+Smax*Cepo(T-Tp)/(SC50+Cepo(T-Tp))
HCtR=1+Smax*Cepo(T-Tp-Tr)/(SC50+Cepo(T-Tp-Tr))
XP(1)=kin*HCtP-kin/100*HCtR
Return
End
Subroutine OUTPUT(Y,T,X)
Implicit None
Include 'globals.inc'
Include 'model.inc'
Real*8 Y(MaxNOE),T,X(MaxNDE)
Real*8 kin,R0,Smax,SC50,Tr,Tp,lambda,HCt0,HCtP,
Real*8 HCtR,Cepo
Smax=P(1)
SC50=P(2)
Tp=P(3)
Tr=P(4)
kin=P(5)
HCt0=1+Smax*Cepo(0.0)/(SC50+Cepo(0.0))
R0=Tr*kin*HCt0
Y(1)=X(1)+R0
Return
End
```

Reticulocyte Response Described by the LIDR Model with the Dornhorst Lifespan Distribution

```
Subroutine DIFFEQ(T,X,XP)
Implicit None
Include 'globals.inc'
Include 'model.inc'
Real*8 T,X(MaxNDE),XP(MaxNDE)
Real*8 kin,R0,Smax,SC50,Tr,Tp,lambda,HCt0,HCtP,
Real*8 HCtR,Cepo,X20
Smax=P(1)
SC50=P(2)
Tp=P(3)
```

```
Tr=P(4)
lambda=P(5)
kin=P(6)
HCt0=1+Smax*Cepo(0.0)/(SC50+Cepo(0.0))
HCtP=1+Smax*Cepo(T-Tp)/(SC50+Cepo(T-Tp))
HCtR=1+Smax*Cepo(T-Tp-Tr)/(SC50+Cepo(T-Tp-Tr))
R0=Tr*kin*HCt0
X20=R0/Tr/lambda*(1-EXP(-lambda*Tr))
XP(1)=kin*HCtP-kin*HCtR*EXP(-lambda*Tr)
-lambda*(X(2)+X20)
XP(2)=kin*HCtP-kin*HCtR*EXP(-lambda*Tr)
-lambda*(X(2)+X20)
Return
End
```

```
Subroutine OUTPUT(Y,T,X)
Implicit None
Include 'globals.inc'
Include 'model.inc'
Real*8 Y(MaxNOE),T,X(MaxNDE)
Real*8 kin,R0,Smax,SC50,Tr,Tp,lambda,
Real*8 HCt0,Cepo
Smax=P(1)
SC50=P(2)
Tp=P(3)
Tr=P(4)
lambda=P(5)
kin=P(6)
HCt0=1+Smax*Cepo(0.0)/(SC50+Cepo(0.0))
R0=Tr*kin*HCt0
Y(1)=X(1)+R0
Return
End
```

Reticulocyte Response Described by the LIDR Model with the Gamma Lifespan Distribution

```
Subroutine DIFFEQ(T,X,XP)
Implicit None
Include 'globals.inc'
Include 'model.inc'
Real*8 T,X(MaxNDE),XP(MaxNDE)
Real*8 kin,R0,Ttrans,Ncom,Smax,SC50,Tr,Tp,SD,HCt0
```

```
Real*8 HCtP,Cepo
Integer N,M,Ntrans
Smax=P(1)
SC50=P(2)
Tp=P(3)
Ttrans=P(4)
Ncom=P(5)
kin=P(6)
Tr=Ncom*Ttrans
SD=SQRT(Ncom)*Ttrans
Ntrans=INT(Ncom)
M=Ntrans+1
HCt0=1+Smax*Cepo(0.0)/(SC50+Cepo(0.0))
HCtP=1+Smax*Cepo(T-Tp)/(SC50+Cepo(T-Tp))
XP(1)=kin*HCtP - (X(2)+kin*HCt0)
Do N=2,M-1
XP(N)=(X(N+1)-X(N))/Ttrans
ENDDO
XP(M)=(kin*HCtP - (X(M)+kin*HCt0))/Ttrans
Return
End


Subroutine OUTPUT(Y,T,X)
Implicit None
Include ''globals.inc''
Include ''model.inc''
Real*8 Y(MaxNOE),T,X(MaxNDE)
Real*8 kin,R0,Ttrans,Ncom,Smax,SC50,Tr,Tp,HCt0,Cepo
Smax=P(1)
SC50=P(2)
Tp=P(3)
Ttrans=P(4)
Ncom=P(5)
kin=P(6)
Tr=Ncom*Ttrans
HCt0=1+Smax*Cepo(0.0)/(SC50+Cepo(0.0))
R0=Tr*kin*HCt0
Y(1)=X(1)+R0
Return
End
```

Reticulocyte Response Described by the LIDR Model with the Lognormal Lifespan Distribution

```
Subroutine DIFFEQ(T,X,XP)
Implicit None
Include 'globals.inc'
Include 'model.inc'
Real*8 T,X(MaxNDE), XP(MaxNDE)
Real*8 Tlast,dtau,sum,alpha(100),ss,Tp,Smax,Sigma
Real*8 SC50,m,Tmean, Cepo,kin,R0
Real*8 mp,pi,Taui,HCt0,HCtP,HCtT
Integer N,i
Smax=P(1)
SC50=P(2)
Tp=P(3)
m=P(4)
sigma=P(5)
kin=P(6)
N=100
Tlast=350.0
dtau=Tlast/N
pi=4.0d0*dATAN(1.0d0)
sum=0.0
Do i=1,N
mp=(i-0.5)*dtau
alpha(i)=1/(sigma*mp*(2*pi)**0.5)*exp(-(log(mp)-m)**
2/(2*sigma**2))
sum=sum+alpha(i)*dtau
Enddo
Tmean=0.0
Do i=1,N
Tmean=Tmean+0.5*alpha(i)/sum*(i**2-(i-1)**2)*dtau**2
Enddo
HCt0=1+Smax*Cepo(0.0)/(SC50+Cepo(0.0))
HCtP=1+Smax*Cepo(T-Tp)/(SC50+Cepo(T-Tp))
ss=0.0
Do i=1,N
ss=ss+alpha(i)/sum*(X(i+1)-X(i)+kin*HCt0*dtau)
Enddo
Do i=1,N+1
Taui=(i-1)*dtau
HCtT=1+Smax*Cepo(t-Tp-Taui)/(SC50+Cepo(t-Tp-Taui))
```

```
XP(i)=kin*HCtP-kin*HCtT
Enddo
XP(N+2)=kin*HCtP - ss
Return
End

Subroutine OUTPUT(Y,T,X)
Implicit None
Include 'globals.inc'
Include 'model.inc'
Real*8 Y(MaxNOE),T,X(MaxNDE)
Real*8 Tlast,dtau,sum,alpha(100),ss,Tp,Smax,Sigma,
Real*8 SC50,m,Tmean,Cepo,kin,R0
Real*8 mp,pi,Taui,HCt0,HCtP,HCtT
Integer N,i
Smax=P(1)
SC50=P(2)
Tp=P(3)
m=P(4)
sigma=P(5)
kin=P(6)
N=100
Tlast=350.0
dtau=Tlast/N
pi=4.0d0*dATAN(1.0d0)
sum=0.0
Do i=1,N
mp=(i-0.5)*dtau
alpha(i)=1/(sigma*mp*(2*pi)**0.5)*exp(-(log(mp)-m)
**2/(2*sigma**2))
sum=sum+alpha(i)*dtau
Enddo
Tmean=0.0
Do i=1,N
Tmean=Tmean+0.5*alpha(i)/sum*(i**2-(i-1)**2)*dtau**2
Enddo
HCt0=1+Smax*Cepo(0.0)/(SC50+Cepo(0.0))
R0=Tmean*kin*HCt0
Y(1)=X(N+2)+R0
Return
End
```

GLOSSARY

$\alpha_1, \ldots, \alpha_n$	values of the lognormal p.d.f. at the histogram bin midpoints
$a_1, \ldots, a_n$	heights of histogram p.d.f. bars
a, b	variance parameters
$C, C(t)$	drug concentration in plasma
$C_{\mathrm{EPO}}(t)$	rHuEPO serum concentration
C_0, C_1, C_2	coefficients in equation for $C_{\mathrm{EPO}}(t)$
$C_{\mathrm{del}}(t)$	$C_{\mathrm{EPO}}(t)$ delayed by T_P
$\Delta\tau$	lifespan increment; width of a bin in the lifespan histogram
Δt	time increment
$\delta(t - T_P)$	Dirac delta function.
$E_{\max}$	maximum effect
EC_{50}	drug concentration eliciting 50% of maximum effect
$k_{\mathrm{in}}(t)$	cell (response) production rate
$k_{\mathrm{out}}(t)$	cell (response) elimination rate
$k_{\mathrm{in}} * \ell(t)$	convolution of k_{in}(t) with $\ell(\tau)$
$k_{\mathrm{in0}}, k_{\mathrm{in}R}$	cell (response) production rate in the absence of drug
k_1, k_2	coefficients in equation for C_{EPO}(t)
k_{el}	first-order elimination rate constant of drug from plasma
$\ell, \ell(\tau)$	probability density function for lifespan distribution
λ	first-order random destruction constant
LIDR	lifespan based indirect response
M	number of cells in the precursor pool
M_0	baseline cell number in the precursor pool
MPE	mean prediction percent error
m	parameter in the lognormal distribution
N	number of cells in the central pool
N_0	baseline cell number in the central pool
PK/PD	pharmacokinetic/pharmacodynamic
$P(\tau \leq t)$	probability of $\tau \leq t$
p.d.f.	probability density function
R	response variable
R_0	baseline response
RMSPE	root mean squared prediction percent error

RBC	red blood cells
rHuEPO	recombinant human erythropoietin
σ	parameter in the lognormal distribution
$S_{\max}$	maximum stimulatory effect
SC_{50}	drug concentration eliciting 50% of maximum stimulatory effect
SD	standard deviation
SD_{RET}	SD for reticulocyte lifespan
$\theta(t)$	Heaviside jump function
τ	lifespan
τ_0	transient time in the gamma p.d.f.
$\tau_1, \ldots, \tau_n$	bin limits in the histogram p.d.f.
T_R	senescence lifespan in the Dornhorst p.d.f.
T_{RET}	mean reticulocyte lifespan
T	mean lifespan
t	time
t_{lag}	time lag for $C_{\mathrm{EPO}}(t)$
V	plasma compartment volume
V_c	volume of the central cell pool
$Var(Y)$	variance of variable Y
$X_1, \ldots, X_n$	dummy variables used to calculate the convolution integral
Y	model prediction variable

REFERENCES

1. L. A. Harker, L. K. Roskos, U. M. Marzec, R. A. Carter, J. K. Cherry, B. Sundell, E. N. Cheung, D. Terry, and W. Sheridan. Effects of megakaryocyte growth and development factor on platelet production, platelet lifespan, and platelet function in healthy human volunteers. *Blood* **95**:2514–2522 (2000).
2. L. E. Friberg, A. Freijs, M. Sandstrom, and M. O. Karlsson. Semiphysiological model for the time course of leukocytes after varying schedules of 5-fluorouracil in rats. *J. Pharmacol. Exp. Ther.* **295**:734–740 (2000).
3. A. G. McKendrick. Application of mathematics to medical problems. *Proc. Edinburgh Math. Soc.*, **44**:98–130 (1926).
4. H. Von Foerster. Some remarks on changing populations. In: F. Stohlman (ed.), *The Kinetics of Cellular Proliferation*. Grune & Stratton, New York, 1959.
5. J. Belair, M. C. Mackey, and J. M. Mahaffy. Age-structured and two-delay models for erythropoiesis. *Math. Biosci.* **128**:317–346 (1995).
6. W. Krzyzanski, R. Ramakrishnan, and W. J. Jusko. Basic models for agents that alter production of natural cells. *J. Pharmacokin. Biopharm.* **27**:467–489 (1999).
7. P. Veng-Pedersen, S. Chapel, P. R. L. Schmidt, N. H. Al-Huniti, R. T. Cook, and J. A. Widness. An integrated pharmacodynamic analysis of erythropoietin, reticulocyte, and hemoglobin responses in acute anemia. *Pharm. Res.* **19**:1630–1634 (2002).

8. N. I. Berlin and P. D. Berk. The biological life of the red cell. In: DM. Surgenor (ed.), *The Red Blood Cells.*, vol. II, Academic Press, New York, 1975.
9. J. M. Paulus. Measuring mean life span, mean age and variance of longevity in platelets. In: J. M. Paulus (ed.), *Platelet Kinetics, Radioisotopic, Cytological, Mathematical, and Clinical Aspects*, North-Holland Publishing Company, Amsterdam, 1971.
10. A. C. Dornhorst. The interpretation of red cell survival curves. *Blood* **6**:1284–1292 (1951).
11. P.-E. E. Bergner. On stochastic interpretation of cell survival curves. *J. Ther. Biol.* **2**: 279–295 (1962).
12. I. Branehog, B. Ridell, and A. Weinfeld. On the analysis of platelet survival curves and the calculation of platelet production and destruction. *Scand. J. Haematol.* **19**:230–241 (1977).
13. ICSH, Recommended methods for radioisotope red-cell survival studies. *Br. J. Haematol.* **45**:659–666 (1980).
14. J. M. Paulus. *Platelet Kinetics, Radioisotopic, Cytological, Mathematical, and Clinical Aspects*. North-Holland Publishing Company, Amsterdam, 1971.
15. E. A. Murphy and M. E. Francis. The estimation of blood platelet survival. I. General principles of the study of cell survival. *Thrombos. Diathes. Haemorrh.* (Stuttg.), **22**:281–295 (1969).
16. E. A. Murphy and M. E. Francis. The estimation of blood platelet survival. II. The multiple hit model. *Thrombos. Diathes. Haemorrh*. (Stuttg.), **25**:53–80 (1971).
17. D. E. Uehlinger, F. A. Gotch, and L. B. Sheiner. A pharmacodynamic model of erythropietin therapy for uremic anemia. *Clin. Pharmacol. Ther.* **51**:76–89 (1992).
18. N. L. Dayneka, V. Garg, and W. J. Jusko. Comparison of four basic models of indirect pharmacodynamic responses. *J. Pharmacokinet. Biopharm.* **21**:457–478 (1993).
19. P. Veng-Pedersen. Curve fitting and modeling in pharmacokinetics and some practical experiences with NONLIN and a new program FUNFIT. *J. Pharmacokinet. Biopharm.* **5**:513–531 (1977).
20. W. K. Cheung, B. L. Goon, M. C. Guilfoyle, and M. C. Wacholtz. Pharmacokinetics and pharmacodynamics of recombinant human erythropoietin after single and multiple subcutaneous doses to healthy subjects. *Clin. Pharmacol. Ther.* **64**:412–423 (1998).
21. D. Z. D'Argenio and A. Schumitzky. A program package for simulation and parameter estimation in pharmacokinetics. *Comp. Prog. in Biomed.* **9**:115–134 (1979).
22. H. Cramer. *Mathematical Methods of Statistics*, Princeton University Press, Princeton, 1999.
23. L. B. Sheiner and S. L. Beal, Some suggestions for measuring predictive performance. *J. Pharmacokin. Biopharm.* **9**:503–512 (1981).
24. O. Sowade, B. Sowade, K. Brilla, W. Franke, P. Stephan, J. Gross, P. Scigalla, and H. Warnke. Kinetics of reticulocyte maturity fractions and indices and iron status during therapy with epoetin beta (recombinant human erythropoietin) in cardiac surgery patients. *Am. J. Hematol.* **55**:89–96 (1997).
25. H. Akaike. A new look at the statistical model identification. *IEEE Trans Automat Control* AC **19**:716–723 (1974).
26. Y.-N. Sun and W. J. Jusko. Transit compartments vs. gamma distribution function to model signal transduction process in pharmacodynamics. *J. Pharm. Sci.* **87**:732–737 (1998).
27. W. Krzyzanski, J. Dmochowski, N. Matsushima, and W. J. Jusko. Assessment of intra-individual variability in estimation of parameters for basic indirect response models. *AAPS PharmSci.* **5**(4):T2349 (2003).
28. J. J. P. Ruixo, H. C. Kimko, A. C. Chow, V. Piotrovsky, W. Krzyzanski, and W. J. Jusko. Population cell lifespan models for effects of drugs following indirect mechanism of action. *J. Pharmacokin. Pharmacodyn.* **32**:767–793 (2005).
29. M. Kimmel, A. Grossi, J. Amuasi, and A. M. Vannucchi. Non-parametric analysis of platelet lifespan. *Cell Tissue Kinet.* **23**:191–202 (1990).
30. R. Ramakrishnan, W. K. Cheung, M. C. Wacholtz, N. Minton, and W. J. Jusko. Pharmacokinetic and pharmacodynamic modeling of recombinant human erythropoietin

after single and multiple doses in healthy volunteers. *J. Clin. Pharmacol*. **44**:991–1002 (2004).
31. W. Krzyzanski, W. J. Jusko, M. C. Wacholtz, N. Minton, and W. K. Cheung. Pharmacokinetic and pharmacodynamic modeling of recombinant human erythropoietin after multiple subcutaneous doses in healthy subjects. *Eur. J. Pharm. Sci*. **26**:295–306 (2005).